IOSR Journal of Engineering (IOSRJEN) **www.iosrjen.org**
ISSN (e): 2250-3021, ISSN (p): 2278-8719
Vol. 12, Issue 2, February. 2022, || Series -I || PP 11-20

CFD Validation for Laminar and Turbulent Natural Convection in Air-Filled Square Cavity for Applications of Solar Thermal Energy

M. M. Kamal[1], A. M. Taher[2], and A. T. Mahmoud[3]
[1]Professor, [2] Associate Professor, [3]Researcher, Mechanical Power Dept.,
Corresponding Author: A. T. Mahmoud
Faculty of Engineering, Ain Shams University, Cairo, Egypt
Received 28 February 2022; Accepted 29 March 2022

Abstract:
CFD simulations were done using ANSYS Fluent 2021 for a square cavity filled with air to study the laminar as well as the turbulent heat transfer process developing inside the cavity. For the turbulent case, $k-\varepsilon$, $k-\omega\, standard$ and $k-\omega\, SST\, models$ were used. The results of Fluent model were compared with the experimental results given in the literature. The results show that using CFD is a promising method to predict the intricate heat transfer and natural convection occurring inside the cavity. The figures and tables show a good agreement with the experimental results. Each figure shows the comparison of either the velocity or the temperature profile with the benchmark data while the tables show the comparison of the Nusselt number with the Experimental Nusselt.
Keywords: CFD, laminar Natural convection, Turbulent Natural convection, square cavity.

I. INTRODUCTION

Atria are enclosed spaces commonly used nowadays in the design of modern buildings. As such, the intricate heat transfer process inside enclosed cavities is governed by turbulent natural convection and radiation that lead to thermal stratification. Atria can include large glazed areas used for the purpose of lighting and sometimes ventilation as well. If poorly designed, they can cause undesired heat loss and gains resulting in increasing the heating and cooling loads. In contrast, if correctly designed, they can lead to the reduction of energy consumption. Computational fluid dynamics (CFD) has the potential to simulate the fluid flow and heat transfer process of the system desired. CFD model needs the domain to be discretized before it can solve the governing equations of the system. Gan et al. [1] simulated three room types using a CFD package called VORTEX. This study concluded that the CFD package successfully simulated the flows in rooms. Awbi [2] published a paper outlining the study of the temperature and wind speed of the atrium. The study was done using VORTEX CFD package. Gan et al. [3] investigated the effects of an atrium's opening location on the heat transfer process using FLUENT CFD package.

The results of the previous studies were not validated against any experimental data. Another problem is using small-scale models to get the experimental data. As the atrium dimensions get smaller, the Rayleigh number are reduced resulting in the developed stratification and turbulent structures not properly representing those in the full-scale systems. To solve such an issue, the fluid used in the experiments has to be denser [4]. Henkes et al. [5], Sharif et al. [6], and Wen et al. [7] took into consideration validations of turbulent natural convection using different CFD packages. Rundle et al. [8] published a paper criticizing the traditional building energy simulation programs as they cannot predict the behavior of complex heat transfer problems containing turbulent natural convection, radiative heat transfer, and conjugate heat transfer such as atria. They successfully used CFD to simulate the problem and validate it against experimental results to establish the accuracy of the predictions. Ganguli et al. [9] performed CFD simulations for cavities that vary in temperature to find A good agreement of Nusselt number (±10%) between the CFD predictions and the literature data.

There are various turbulence models that can be used in the simulations of the turbulent natural convection in the cavities. Choosing the right model depends on the desired time of simulation and accuracy. The models include: $k-\varepsilon\, model$, $k-\omega\, standard\, model$ and finally $k-\omega\, SST\, model$. For the $k-\varepsilon\, model$, walsh et al. [10] preferred the standard $k-\varepsilon\, model$ more than the complicated ones as it has less computational time. The $k-\omega\, standard\, model$ is a commonly used model that occasionally forms the basis of the SST model. The SST model is a combination of the previous $k-\varepsilon$ and $k-\omega$ models and can switch between the two models based on the turbulent variable. Yingchun Ji [11] compared four eddy viscosity turbulence models to predict the natural convection heat transfer inside air cavities. The results of the CFD simulations were compared to the experimental ones to reveal that the $k-\omega$ results are the closest to the experimental ones. Tobias [12] studied a 2D model of a differentially heated cavity using CFD package CFX-5. The study concluded that the $k-\omega$ standard and SST models has the closest results compared to the experimental results. He also made further studies on the 3D case of the cavity using the $k-\omega$ and SST models. The 3D study suggested that these deviations from measurements were caused by the close proximity of the symmetry planes which inhibited 3D dissipation of turbulence effects of the flow. Aounallah [13] studied a turbulent natural convection developed in a confined cavity up to Rayleigh number of 10^{12}. Among the Reynolds-Averaged Navier-Stokes (RANS) Equations and Models, the Low-Reynold's SST model is superior to other models in predicting the heat transfer inside the cavity. Although this model slightly under-predicted the turbulence quantities, it was able to reproduce the other thermal and physical flow features of the natural convection phenomenon.

In the current study, an investigation of a laminar as well as a turbulent natural convection inside a cavity was performed using ANSYS Fluent 2021 CFD package. The Nusselt number and velocity profiles are validated against either experimental or analytical data. The previously mentioned three turbulence model were compared and comprehensive information about their accuracy was provided.

II. CFD MODEL

2.1 Geometry

In the current study, an air-filled square cavity whose horizontal walls are adiabatic, and the vertical ones are at a constant temperature was studied. The cavity dimensions are manipulated to adjust the Rayleigh number to reach 10^4 and 1.58×10^9 for laminar and turbulent flows, respectively. The dimension of the cavity is 40 mm and 75 mm for laminar and turbulent cases, respectively. Figure 1 shows the geometry of the cavity for both the cases.

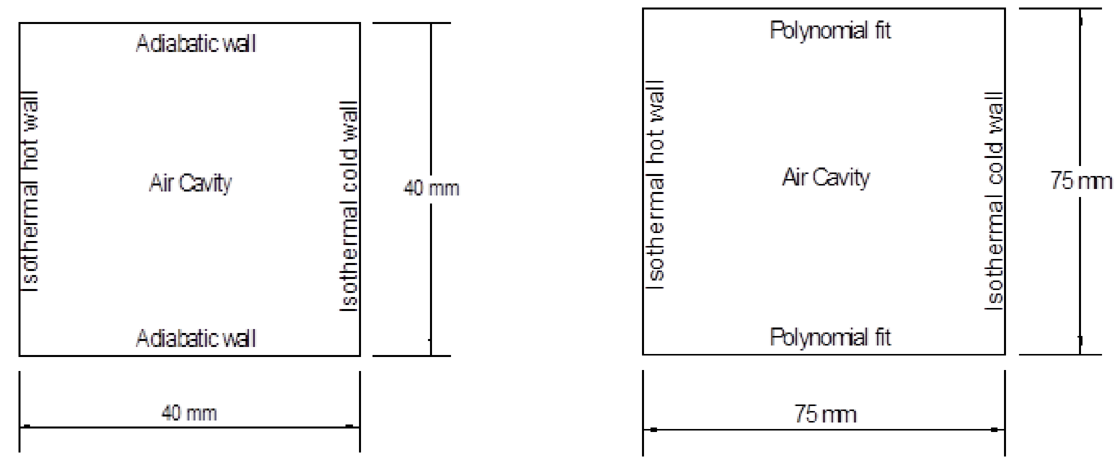

Figure 1. The cavities for the turbulent and laminar cases respectively

2.2 Air Properties

The film temperature was taken as an average temperature of 25°C, and the Boussinesq approximation was used. The thermophysical properties of air are described in Table 1.

Table 1. Thermophysical properties of air for both laminar and turbulent cases

Density	1.184 (kg/m^3)
Thermal Expansion	0.00338 (K^{-1})
Kinematic Viscosity	15.52×10^{-6} (m^2/s)
Thermal Diffusivity	22.39×10^{-6} (m^2/s)
Dynamic viscosity	18.37×10^{-6} (N s /m^2)
Thermal conductivity	0.02624 (W / m K)
Specific heat	1006 (J/Kg K)

2.3 Governing Equations

The main equations which are used by ANSYS Fluent include: conservation of mass, conservation of momentum, and conservation of energy. These governing equations are discretized by ANSYS CFD solver to numerically get the desired parameters at each node and along the wished period.

Conservation of mass:

$$\frac{\partial \rho}{\partial t} + \nabla . (\rho \vec{v}) = 0 \qquad [1]$$

Conservation of momentum:

$$\frac{\partial}{\partial t} (\rho \vec{v}) + \nabla . (\rho \vec{v} \vec{v}) = -\nabla p + \nabla . (\bar{\bar{\tau}}) + \rho g \qquad [2]$$

Conservation of energy:

$$\frac{\partial}{\partial t} (\rho C_p T) + \nabla . (\rho C_p T \vec{v}) = \nabla . (\mathrm{k} \nabla \mathrm{T}) \qquad [3]$$

In addition to the three main governing equations, there are the turbulence model equations.

2.4 Boundary and Initial Conditions

1. Validation of Laminar Case

Both the top and bottom walls are considered adiabatic with the no-slip condition. The right wall was fixed at $T_c = 24.196^oC$ with no-slip wall condition, and the left wall was fixed at $T_h = 25.804^oC$ with no-slip wall condition.

2. Validation of Turbulent Case

The temperature of the top and bottom walls is a Polynomial fit of the experimental data obtained by Ampofo [14]. The polynomial fit equations were as follows:

$\Theta_{top} = -7.37717\ X^5 + 16.9338\ X^4 - 15.7646\ X^3 + 7.325\ X^2 - 2.0199\ X + 0.96582$

$\Theta_{bottom} = 7.739\ X^6 - 31.356\ X^5 + 48.281\ X^4 - 37.512\ X^3 + 16.094\ X^2 - 4.191\ X + 0.95288$

where, $\Theta = (T-T_c)/(T_h-T_c)$, $X = x/L$

The right wall was fixed at $T_c = 10^oC$ with no-slip wall condition, and the left wall was fixed at $T_h = 50^oC$ with no-slip wall condition.

2.5 Mesh and Mesh Independence Test

A non-uniform expanding grid with a bias factor was used to refine the cells near the wall in order to capture the physics near the wall accurately. Figure 2 shows the mesh of size 160 x 160 applied to the cavity.

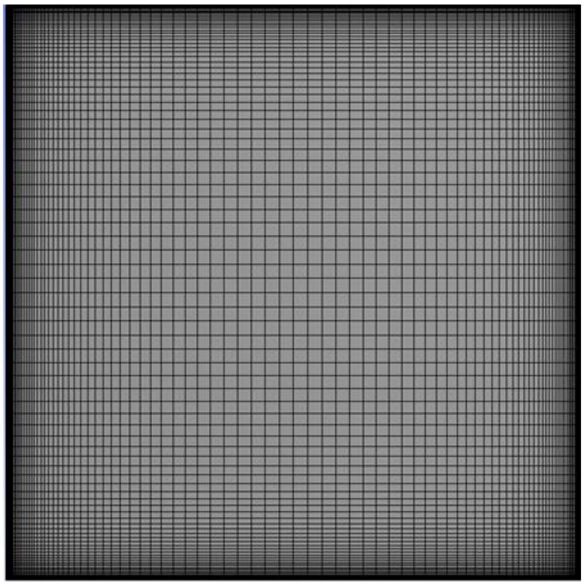

Figure 2. The mesh of size 160 x 160 applied to the cavity, the turbulent case

Mesh independence test is necessary to determine the cell size at which the results start to approach the experimental results of De Vahl Davis [14] and the numerical results of Sarafraz [15] for the laminar study. The test was done on six cases ranging in number of nodes per side from 20 to 200. From Figure 3 and Table 2 it was noticed that starting from 80 nodes per side the error was equal or below 0.2% and it reached zero at size of 160 x 160. That is why the size of the cell is chosen to be 0.5 mm for both laminar and turbulent validation cases. It is noted that the Nusselt number is calculated using the following: $\overline{Nu} = \frac{q\,L}{k\,(T_h - T_c)}$ where q: is the heat transfer rate (W/m^2), L: cavity dimension, k: Thermal fluid conductivity. Experimental average Nusselt Number of De Vahl Davis is equal to 2.24.

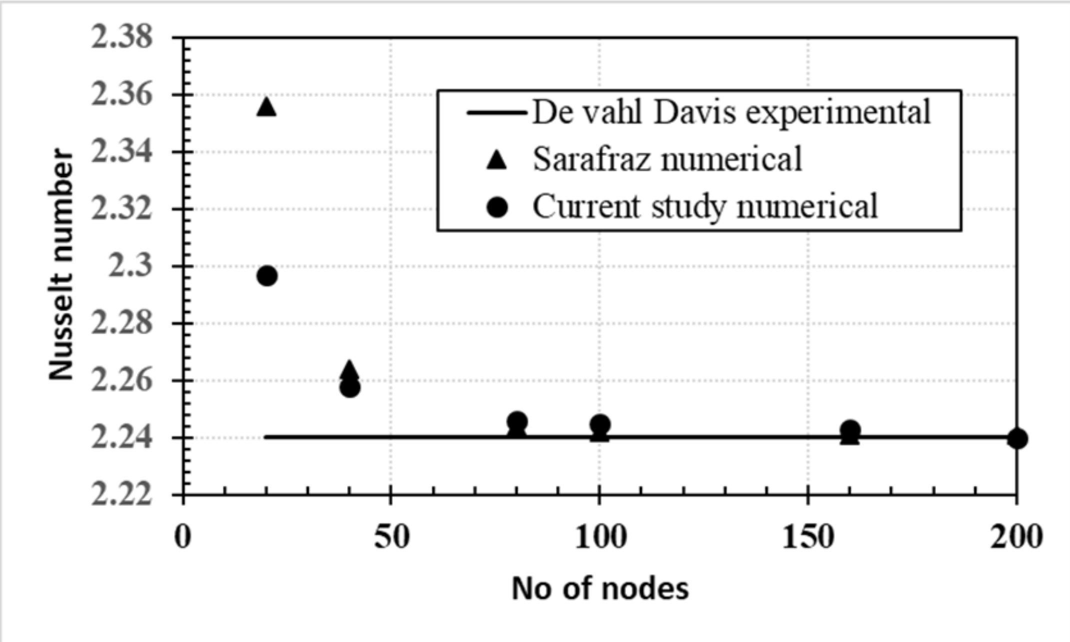

Figure 3. Resulted Nusselt number for different mesh sizes for air-filled square cavity laminar case

Table 2. Nusselt of current study versus Sarafraz's results for air-filled square cavity laminar case

No of nodes per side	Sarafraz simulation results [15]	% Error	Current study results	% Error
20	2.356	5.2%	2.297	2.54%
40	2.264	1.1%	2.258	0.8 %
80	2.244	0.2%	2.246	0.26 %
100	2.242	0.1%	2.245	0.22 %
160	2.241	0.0%	2.243	0.13%
200	2.241	0.0%	2.24	0.00 %

III. RESULTS AND DISCUSSION

3.1 Validation of Laminar Case

Figures 4 and 5 show the temperature and velocity contours of the air cavity. The temperature contour shows a gradient in temperature between the cold and the hot walls as expected.

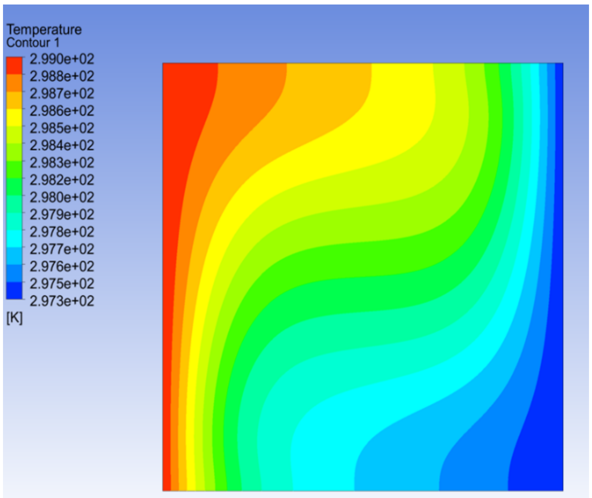

Figure 4. Temperature contours for air-filled square cavity - laminar case

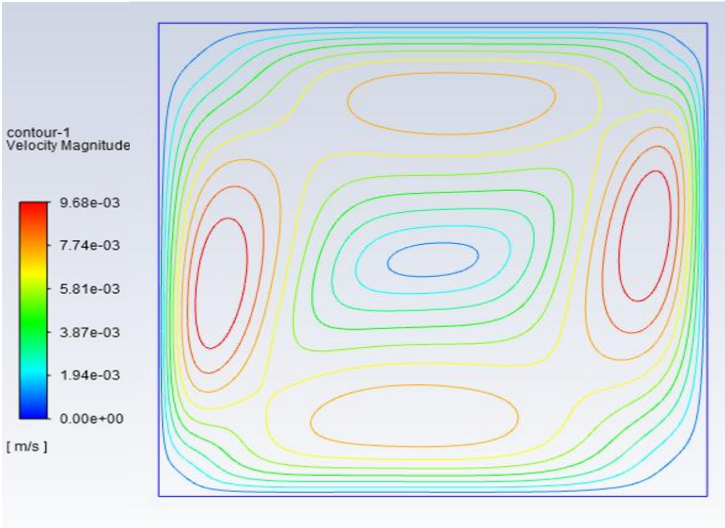

Figure 5. Velocity contours for air-filled square cavity - laminar case

To validate the dimensionless velocity and temperature profiles of the laminar case, another simulation was done for a cavity having a side length of 42.6 mm and a film temperature of 20^{o}C. The results from ANSYS Fluent showed good agreement with the results by Krane and Jesee [16]. Figures 6 and 7 show the dimensionless temperature and velocity comparisons respectively for the laminar case. They show good agreement with the results of Krane and Jesee.

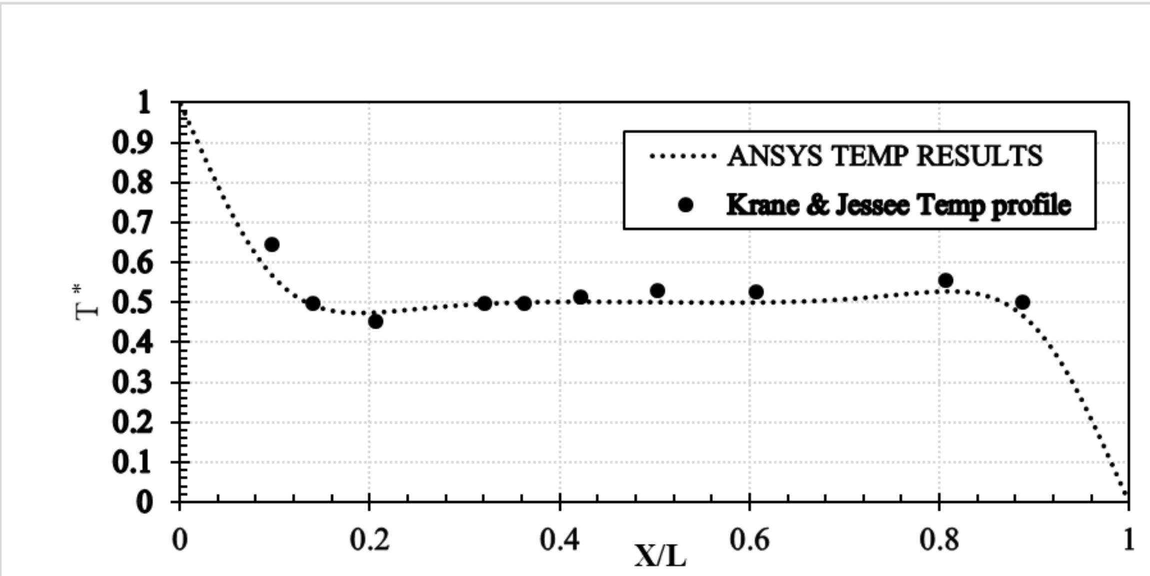

Figure 6. Dimensionless temperature profile for air-filled square cavity laminar case

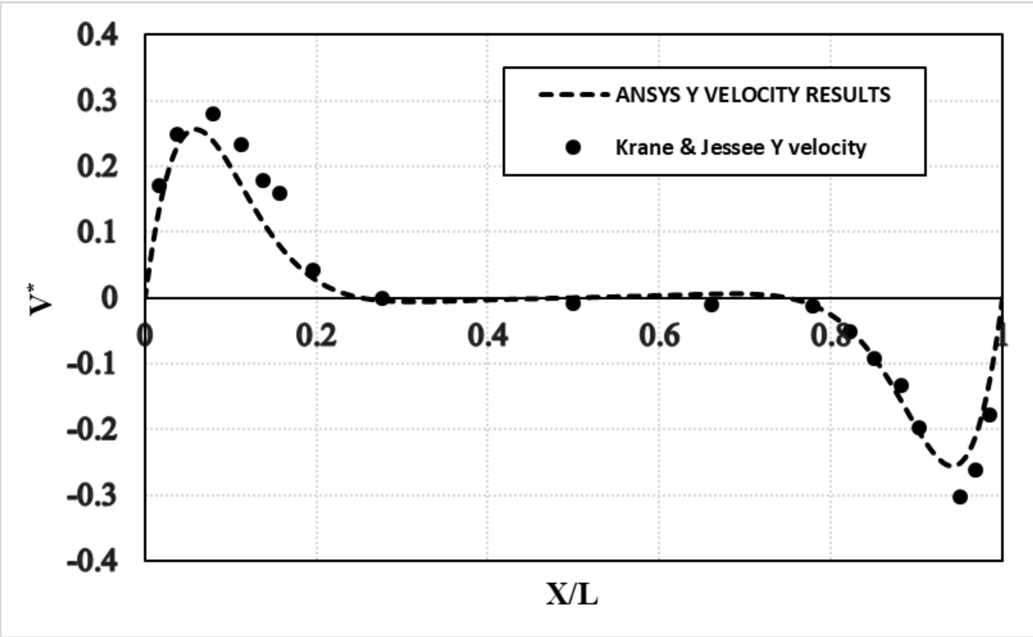

Figure 7. Dimensionless velocity profile for air-filled square cavity laminar case

3.2 Validation of Turbulent Case

Velocity and temperature profiles were compared to those experimental results of Ampofo [17]. The Nusselt number was compared to the experimental results of Ampofo [17] and the numerical results of Rundle [8]. The full buoyancy option was used to account for the generation of turbulent kinetic energy due to buoyancy. Table 3 through Table 5 show a comparison of the average Nusselt Number. Three models were used for the comparison which are: $k-\ \omega$ standard , $k-\ \omega$ SST and $k-\ \varepsilon$.

The tables show that the average deviation of Nusselt number of the $k-\ \omega$ standard, $k-\ \omega$ SST and $k-\ \varepsilon$ are 12.7 %, 8.35 % and 15.57%, respectively. The deviation of the current study in the Nusselt number was better than those produced from the study of Rundle [17]. $k-\ \omega$ SST model was the best to predict the Nusselt number. The large errors in the top and bottom walls are related to the fact that the polynomial fit is not precise in representing the experimental data. The simulations under predicted the Nusselt Number. Figures 8 to 10 show the comparison of the velocity profile of the current study with Rundle's study.

Table 3. Nusselt number of $k-\ \omega$ standard-turbulent cavity case

$k-\ \omega$ standard							
Experimental		Rundle standard		Rundle production		Rundle Production & dissipation	
Surface	Nu	Nu	Error %	Nu	Error %	Nu	Error %
Hot Wall	62.9	56.94	9.48 %	57.19	9.08 %	58.33	7.27 %
Cold Wall	62.6	57.07	8.83 %	59.36	5.18 %	58.43	6.66 %
Bottom	13.9	8.69	37.48 %	11.25	19.06 %	10.04	27.77 %
Top	14.4	8.62	40.14 %	9.07	37.01 %	9.94	30.97 %
Average			23.98 %		17.58 %		18.17 %
Experimental		Current study standard		Current study production only		Current study Production & dissipation	
Surface	Nu	Nu	Error %	Nu	Error %	Nu	Error %
Hot Wall	62.9	57.3	8.9 %	59.13	6.0 %	59.13	6.0 %
Cold Wall	62.6	57.3	8.5 %	59.0	5.6 %	59.0	5.6 %
Bottom	13.9	10.4	25.5 %	11.3	18.4 %	11.3	18.4 %
Top	14.4	10.3	28.4 %	11.4	20.9 %	11.4	20.9 %
Average			17.8 %		12.7 %		12.7 %

Table 4. Nusselt number of $k-\ \omega$ SST-turbulent cavity case

$k-\ \omega$ SST							
Experimental		Rundle standard		Rundle production		Rundle Production & dissipation	
Surface	Nu	Nu	Error %	Nu	Error %	Nu	Error %
Hot Wall	62.9	55.2	12.24 %	57.54	8.52 %	56.83	9.65 %
Cold Wall	62.6	55.26	11.73 %	57.68	7.86 %	56.87	9.15 %
Bottom	13.9	10.93	21.37 %	11.5	17.27 %	11.36	18.27 %
Top	14.4	10.87	24.51 %	11.35	21.18 %	11.33	21.32 %
Average			17.46 %		13.71 %		14.6 %
Experimental		Current study standard		Current study production only		Current study Production & dissipation	
Surface	Nu	Nu	Error %	Nu	Error %	Nu	Error %
Hot Wall	62.9	55.7	11.4 %	58.5	7.0 %	58.5	7.0 %
Cold Wall	62.6	55.5	11.4 %	58.4	6.8 %	58.4	6.8 %
Bottom	13.9	11.5	17.5 %	12.7	8.7 %	12.7	8.7 %
Top	14.4	11.7	18.6 %	12.8	10.9 %	12.8	10.9 %
Average			14.7 %		8.35 %		8.35 %

Table 5. Nusselt number of $k-\ \varepsilon$ for turbulent cavity case

$k-\ \varepsilon$							
Experimental		Rundle standard (Scalable)		Rundle production (Scalable)		Rundle Production & dissipation (Scalable)	
Surface	Nu	Nu	Error %	Nu	Error %	Nu	Error %
Hot Wall	62.9	24.8	60.57 %	24.1	61.69 %	23.6	62.48 %
Cold Wall	62.6	24.8	60.38 %	24.1	61.5 %	23.6	62.3 %
Bottom	13.9	6.1	56.12 %	4.9	64.75 %	5.3	61.87 %
Top	14.4	5.3	63.19 %	4.7	67.36 %	5.0	65.28 %
Average			60.07 %		63.82 %		62.98 %
Experimental		Current study standard		Current study production only		Current study Production & dissipation	
Surface	Nu	Nu	Error %	Nu	Error %	Nu	Error %
Hot Wall	62.9	52.8	16.1 %	56.12	10.77 %	56.1	10.8 %
Cold Wall	62.6	52.5	16.2 %	55.92	10.67 %	55.9	10.7 %
Bottom	13.9	8.4	39.7 %	11.16	19.71 %	11.2	19.7 %
Top	14.4	8.7	39.7 %	11.36	21.1 %	11.4	21.1 %
Average			27.92%		15.56 %		15.57 %

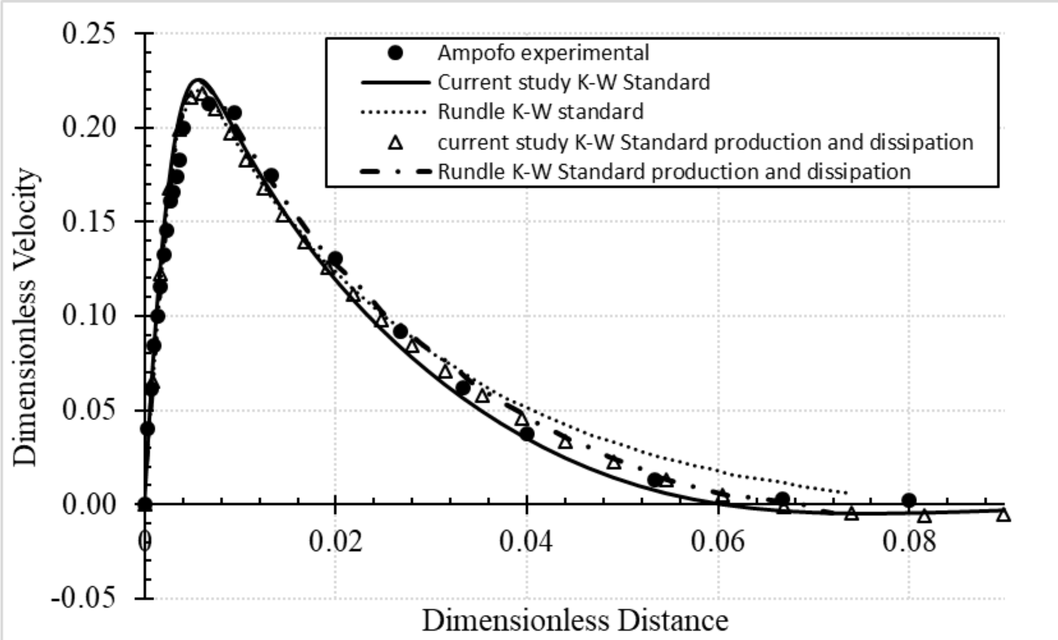

Figure 8. Dimensionless velocity profile for air-filled cavity - turbulent case ($k - \omega$ standard model)

Figure 8 is concerned with the comparison of $k - \omega$ standard. It showed that the current study yielded closer results to the experimental ones than Rundle's results. For the $k - \omega$ SST case, Figure 9 reveals that the use of the full buoyancy model gave the same results as Rundle's. However, when using the low Reynold's correction, it yielded much better results. The low Reynolds correction can produce a delayed onset of the turbulent wall boundary layer and constitute a straightforward model for laminar-turbulent transition. For Figure 10, Rundle used scalable wall functions $k - \varepsilon$ model which did not yield good agreement with the experimental results. However, the current study used enhanced wall treatment which gave better agreement with the results of Ampofo [17]. The scalable wall functions excessively under predicted the maximum velocity which is the top of the velocity profile. Although the results of the current study were satisfactorily close to the experimental results of Ampofo [17], there was slight differences for many reasons. The reasons are that the properties of the air are constant not changing with temperature, the polynomial fits used as boundary conditions are not accurate, and thermal radiation is not modelled in the current study. The turbulent investigation of the air cavity showed that the $k - \omega$ standard is better at predicting the velocity profiles and $k - \omega$ SST is better at predicting the Nusselt Number.

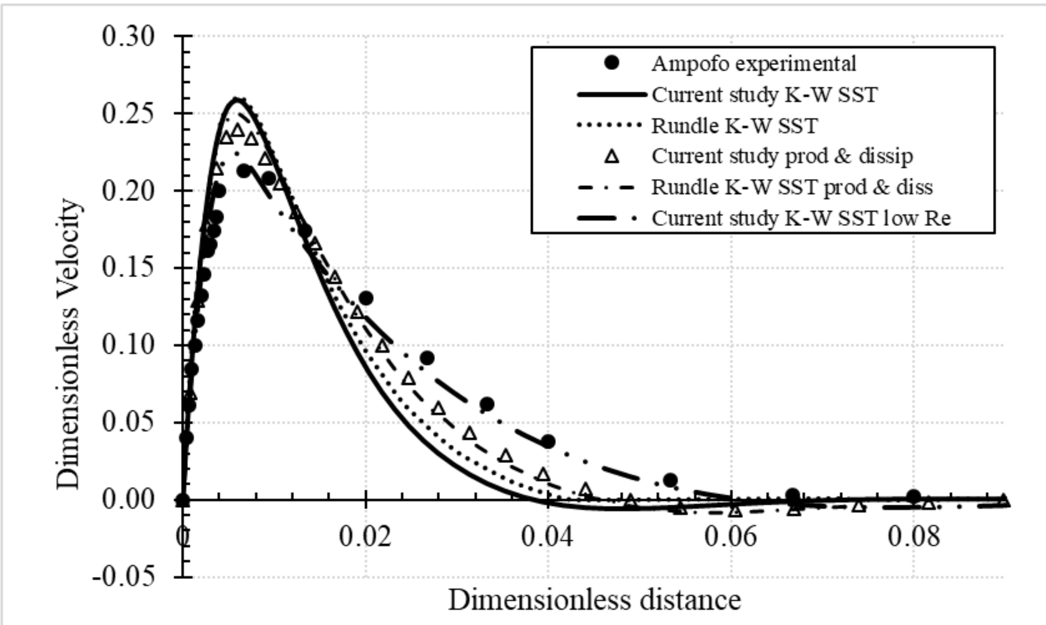

Figure 9. Dimensionless velocity profile for air-filled cavity - turbulent case ($k - \omega$ SST model)

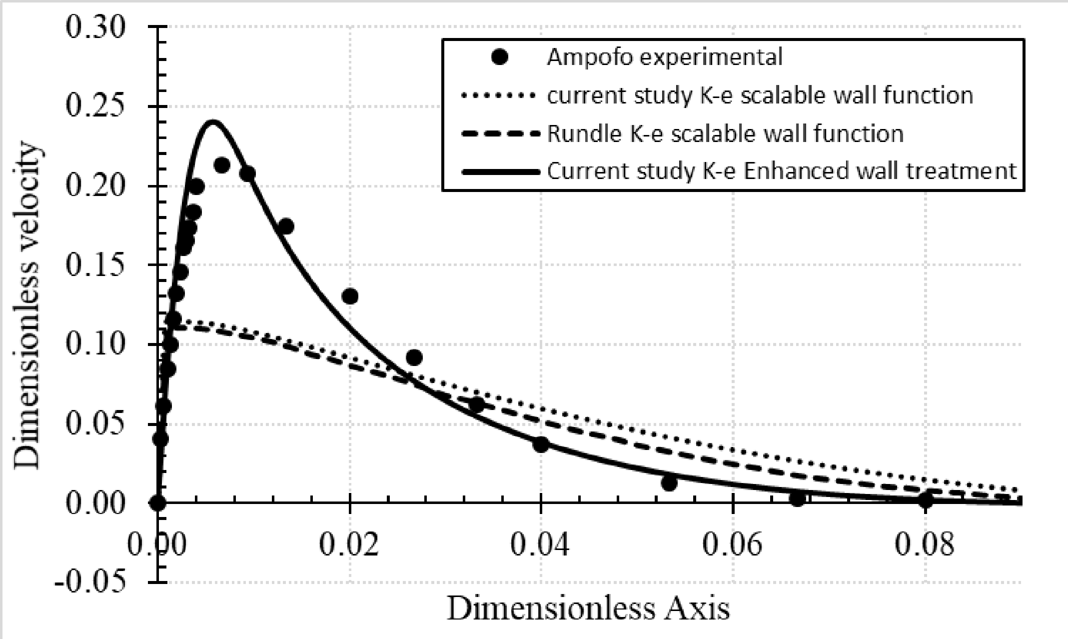

Figure 10. Dimensionless velocity profile for air-filled cavity - turbulent case ($k - \varepsilon$ model)

IV. CONCLUSIONS

A 2D CFD model of an air-filled square cavity was simulated in both laminar and turbulent cases. The vertical walls of the cavity in both cases were isothermal, one at hot temperature another at colder one. The horizontal walls were considered adiabatic at the laminar case while in the turbulent case, a polynomial fit of Ampofo's experimental data [17] is used as a boundary condition for the temperature of the walls to compensate for the heat loss through those walls. The comparison of the velocity profiles showed a promising agreement with the benchmark data while the tables showed that the used models under predicted the Nusselt Number compared to the experimental Nusselt. However, the fact that Nusselt results of the current study were better than that of Rundle's [8] proved that using CFD in predicting the heat transfer for such cases becomes more and more reliable as the CFD packages develop. The good agreement between the results of the current study and the results of the previous work is a main finding of the current research. The study also revealed that the $k - \omega$ standard is better at predicting the velocity profiles while $k - \omega$ SST is better at predicting the Nusselt Number. The current research has constructed and tested a reliable CFD model that can help in solving the problem of predicting the intricate heat transfer inside cavities. The findings of the current study can help future researchers construct the CFD model and choose the right turbulence model for more complex heat transfer problems like energy storages.

Nomenclature

ρ	Density (kg/m^3)
t	Time (s)
$\vec{v}$	Velocity vector (m/s)
C_p	Specific heat capacity under constant pressure (kJ/kg.K)
T	Temperature (K)
k	Thermal conductivity (W/m.K)

REFERENCES

[1]. Gan, G., & Awbi, H. B. (1994). Numerical simulation of the indoor environment. Building and Environment, 29(4), 449-459.
[2]. Awbi, H. B. (1996). Air movement in naturally-ventilated buildings. Renewable energy, 8(1-4), 241-247.
[3]. Gan, G., & Riffat, S. B. (2004). CFD modelling of air flow and thermal performance of an atrium integrated with photovoltaics. Building and Environment, 39(7), 735-748.
[4]. Hassani, A. V., & Hollands, K. G. T. (1989). Prandtl number effect on external natural convection heat transfer from irregular three-dimensional bodies. International journal of heat and mass transfer, 32(11), 2075-2080.

[5]. Henkes, R. A. W. M., & Hoogendoorn, C. J. (1995). Comparison exercise for computations of turbulent natural convection in enclosures. Numerical Heat Transfer, Part B Fundamentals, 28(1), 59-78.
[6]. Sharif, M. A. R., & Liu, W. (2003). Numerical study of turbulent natural convection in a side-heated square cavityat various angles of inclination. Numerical Heat Transfer: Part A: Applications, 43(7), 693-716.
[7]. Wen, J. X., Liu, F., & Lo, S. (2001). Performance comparison of a buoyancy-modified turbulence model with three LRN turbulence models for a square cavity. Numerical Heat Transfer: Part B: Fundamentals, 39(3), 257-276.
[8]. Rundle, C. A., Lightstone, M. F., Oosthuizen, P., Karava, P., & Mouriki, E. (2011). Validation of computational fluid dynamics simulations for atria geometries. Building and Environment, 46(7), 1343-1353.
[9]. Ganguli, A. A., Pandit, A. B., & Joshi, J. B. (2007). Numerical predictions of flow patterns due to natural convection in a vertical slot. Chemical engineering science, 62(16), 4479-4495.
[10]. Walsh, P. C., & Leong, W. H. (2004). Effectiveness of several turbulence models in natural convection. International Journal of Numerical Methods for Heat & Fluid Flow.
[11]. Ji, Y. (2014). CFD modelling of natural convection in air cavities. CFD Letters, 6(1), 15-31.
[12]. Zitzmann, T., Cook, M., Pfrommer, P., Rees, S., & Marjanovic, L. (2005, August). Simulation of steady-state natural convection using CFD. In Proc. of the 9th International IBPSA Conference Building Simulation 2005 (pp. 1449-1456). Montréal: IBPSA.
[13]. Aounallah, M., Addad, Y., Benhamadouche, S., Imine, O., Adjlout, L., & Laurence, D. (2007). Numerical investigation of turbulent natural convection in an inclined square cavity with a hot wavy wall. International Journal of Heat and Mass Transfer, 50(9-10), 1683-1693.
[14]. de Vahl Davis, G., & Jones, I. P. (1983). Natural convection in a square cavity: a comparison exercise. International Journal for numerical methods in fluids, 3(3), 227-248.
[15]. Sarafraz, P. (2014). Thermal optimization of flat plate PCM capsules in natural convection solar water heating systems (Doctoral dissertation).
[16]. Krane, R. J. (1983). Some detailed field measurements for a natural convection flow in a vertical square enclosure. In Proceedings of the First ASME-JSME Thermal Engineering Joint Conference, 1983 (Vol. 1, pp. 323-329).
[17]. Ampofo, F., & Karayiannis, T. G. (2003). Experimental benchmark data for turbulent natural convection in an air filled square cavity. International Journal of Heat and Mass Transfer, 46(19), 3551-3572.

M. M. Kamal, et. al. "CFD Validation for Laminar and Turbulent Natural Convection in Air-Filled Square Cavity for Applications of Solar Thermal Energy." *IOSR Journal of Engineering (IOSRJEN)*, 12(02), 2022, pp. 11-20.